High rate of hypomorphic variants as the cause of inherited ataxia and related diseases: study of a cohort of 366 families

Mehdi Benkirane, Cecilia Marelli, Claire Guissart, Agathe Roubertie, Elizabeth Ollagnon, Ariane Choumert, Frédérique Fluchère, Fabienne Ory Magne, Yosra Halleb, Mathilde Renaud, et al.

High rate of hypomorphic variants as the cause of inherited ataxia and related diseases: study of a cohort of 366 families

Mehdi Benkirane[1], Cecilia Marelli[2], Claire Guissart[1], Agathe Roubertie[3,4], Elizabeth Ollagnon[5], Ariane Choumert[6], Frédérique Fluchère[7], Fabienne Ory Magne[8], Yosra Halleb[1], Mathilde Renaud[9], Lise Larrieu[1], David Baux[1], Olivier Patat[10], Idriss Bousquet[5], Jean-Marie Ravel[9], Danielle Cuntz-Shadfar[3], Catherine Sarret[11], Xavier Ayrignac[12], Anne Rolland[3], Raoul Morales[12], Morgane Pointaux[1], Cathy Lieutard-Haag[1], Brice Laurens[13], Caroline Tillikete[14], Emilien Bernard[14,15], Martial Mallaret[16], Clarisse Carra-Dallière[12], Christine Tranchant[17], Pierre Meyer[3,18], Lena Damaj[19], Laurent Pasquier[19], Cecile Acquaviva[20], Annabelle Chaussenot[21], Bertrand Isidor[22], Karine Nguyen[7], William Camu[12], Alexandre Eusebio[7], Nicolas Carrière[23], Audrey Riquet[24], Eric Thouvenot[25], Victoria Gonzales[12], Emilie Carme[3], Shahram Attarian[7], Sylvie Odent[19], Anna Castrioto[16], Claire Ewenczyk[26], Perrine Charles[26], Laurent Kremer[7], Samira Sissaoui[27], Nadia Bahi-buisson[27], Elsa Kaphan[7], Adrian Degardin[23], Bérénice Doray[28], Sophie Julia[10], Ganaëlle Remerand[29], Valerie Fraix[16], Lydia Abou Haidar[3], Leila Lazaro[30], Vincent Laugel[31], Frederic Villega[32], Cyril Charlin[6], Solène Frismand[9], Marinha Costa Moreira[3], Tatiana Witjas[7], Christine Francannet[11], Ulrike Walther-Louvier[3], Mélanie Fradin[19], Brigitte Chabrol[33], Joel Fluss[34], Eric Bieth[10], Giovanni Castelnovo[25], Sylvain Vergnet[13], Isabelle Meunier[4,35], Alain Verloes[36], Elise Brischoux-Boucher[37], Christine Coubes[38], David Geneviève[38], Nicolas Lebouc[39], Jean Phillipe Azulay[7], Mathieu Anheim[17], Cyril Goizet[40], François Rivier[3,18], Pierre Labauge[12], Patrick Calvas[10] and Michel Koenig[1]✉

PURPOSE: Diagnosis of inherited ataxia and related diseases represents a real challenge given the tremendous heterogeneity and clinical overlap of the various causes. We evaluated the efficacy of molecular diagnosis of these diseases by sequencing a large cohort of undiagnosed families.

METHODS: We analyzed 366 unrelated consecutive patients with undiagnosed ataxia or related disorders by clinical exome-capture sequencing. In silico analysis was performed with an in-house pipeline that combines variant ranking and copy-number variant (CNV) searches. Variants were interpreted according to American College of Medical Genetics and Genomics/Association for Molecular Pathology (ACMG/AMP) guidelines.

RESULTS: We established the molecular diagnosis in 46% of the cases. We identified 35 mildly affected patients with causative variants in genes that are classically associated with severe presentations. These cases were explained by the occurrence of hypomorphic variants, but also rarely suspected mechanisms such as C-terminal truncations and translation reinitiation.

CONCLUSION: A significant fraction of the clinical heterogeneity and phenotypic overlap is explained by hypomorphic variants that are difficult to identify and not readily predicted. The hypomorphic C-terminal truncation and translation reinitiation mechanisms that we identified may only apply to few genes, as it relies on specific domain organization and alterations. We identified *PEX10* and *FASTKD2* as candidates for translation reinitiation accounting for mild disease presentation.

[1]PhyMedExp, Institut Universitaire de Recherche Clinique, UMR_CNRS-Université de Montpellier, INSERM, CHU de Montpellier, Montpellier, France. [2]Expert Centre for Neurogenetic Diseases and Adult Mitochondrial and Metabolic Diseases, Department of Neurology, Gui de Chauliac Hospital, CHU de Montpellier; Molecular Mechanisms of Neurodegenerative Dementia (MMDN), EPHE, INSERM, Université de Montpellier, Montpellier, France. [3]Department of Pediatrics, Gui de Chauliac Hospital, CHU de Montpellier, Montpellier, France. [4]INSERM, Institut des Neurosciences de Montpellier, Montpellier, France. [5]Department of Medical Genetics and Reference Centre for Neurological and Neuromuscular Diseases, Croix-Rousse Hospital, Lyon, France. [6]Department of Rare Neurological Diseases, CHU de la Réunion, Saint-Pierre, France. [7]Department of Neurology, La Timone Hospital, CHU de Marseille, Marseille, France. [8]Department of Neurology, Purpan Hospital, CHU de Toulouse, Toulouse, France. [9]Departments of Genetics and of Neurology, CHU de Nancy, Nancy, France. [10]Department of Clinical Genetics, Purpan Hospital, CHU de Toulouse, Toulouse, France. [11]Department of Medical Genetics, Estaing Hospital, CHU de Clermont-Ferrand, Clermont-Ferrand, France. [12]Department of Neurology, Gui de Chauliac Hospital, CHU de Montpellier, Montpellier, France. [13]Departement of Neurology, Groupe Hospitalier Pellegrin, CHU de Bordeaux, Institute for Neurodegenerative Diseases, CNRS-UMR, Université de Bordeaux, Bordeaux, France. [14]Department of Neurology, Hôpital Neurologique Pierre Wertheimer, Hospices Civils de Lyon, Bron, France. [15]Institut NeuroMyoGène, INSERM-CNRS-UMR, Université Claude Bernard, Lyon, France. [16]Department of Functional Explorations of the Nervous System, CHU de Grenoble, Grenoble, France. [17]Department of Neurology, Hautepierre Hospital, CHU de Strasbourg, Strasbourg, France. [18]PhyMedExp, INSERM, University of Montpellier, CNRS, Montpellier, France. [19]Department of Clinical Genetics, Centre de Référence Maladies Rares Anomalies du Développement, CHU de Rennes, Rennes, France. [20]Department of Hereditary Metabolic Diseases, Centre de Biologie et Pathologie Est, CHU de Lyon et UMR, Bron, France. [21]Department of Medical Genetics, National Centre for Mitochondrial Diseases, CHU de Nice, Nice, France. [22]Department of Medical Genetics, CHU de Nantes, Nantes, France. [23]Department of Neurology, Roger Salengro Hospital, CHU de Lille, Lille, France. [24]Department of Pediatrics Neurology, Roger Salengro Hospital, CHU de Lille, Lille, France. [25]Department of Neurology, CHU de Nîmes, Nîmes, France. [26]Neurogenetics Reference Centre, Hôpital de la Pitié-Salpêtrière, Assistance Publique- Hôpitaux de Paris (AP-HP), Paris, France. [27]Department of Pediatrics, Hôpital Necker-Enfant Malades, Assistance Publique-Hôpitaux de Paris (AP-HP), Paris, France. [28]Department of Medical Genetics, CHU de la Réunion, Saint-Denis, France. [29]Department of Neonatology, Estaing Hospital, CHU de Clermont-Ferrand, Clermont-Ferrand, France. [30]Department of Pediatrics, CH de la Côte Basque-Bayonne, Bayonne, France. [31]Department of Pediatrics, Hautepierre Hospital, CHU de Strasbourg, Strasbourg, France. [32]Department of Pediatrics, Groupe Hospitalier Pellegrin, CHU de Bordeaux; Institute for Interdisciplinary Neurosciences (IINS), CNRS -UMR, Université de Bordeaux, Bordeaux, France. [33]Departement of Pediatrics, La Timone Hospital, CHU de Marseille, Marseille, France. [34]Pediatric Neurology Unit, Geneva Children's Hospital, Genève, Switzerland. [35]Genetics of Sensory Diseases, Gui de Chauliac Hospital, CHU de Montpellier, Montpellier, France. [36]Federation of Genetics, Hôpital Robert Debré, Assistance Publique-Hôpitaux de Paris (AP-HP), Paris, France. [37]Department of Medical Genetics, Hôpital Saint-Jacques, CHU de Besançon, Centre de Génétique Humaine, Université de Franche-Comté, Besançon, France. [38]Department of Medical Genetics, Arnaud de Villeneuve, CHU de Montpellier, Montpellier, France. [39]Department of Neuroradiology, Gui de Chauliac Hospital, CHU de Montpellier, Montpellier, France. [40]Department of Medical Genetics, Pellegrin Hospital, CHU de Bordeaux, Bordeaux, France. ✉email: michel.koenig@inserm.fr

INTRODUCTION

Inherited ataxia/spastic paraplegia (A/SP) and related diseases represent a group of rare neurodegenerative diseases, which are heterogeneous both by their phenotypic manifestations and by the involved physiopathological pathways [1]. The cardinal syndromes, which usually lead to either ataxic or spastic gait may present as a pure form, as a mixed spastic ataxia form, or as part of a complex clinical spectrum with additional neurologic and/or extraneurological symptoms [2, 3]. A/SP may present at any age ranging from infancy to adulthood, and can manifest as dominant, recessive, or X-linked conditions.

To date, more than 400 genes have been identified in dominant and/or recessive forms of inherited A/SP [4, 5]. The mutational spectrum for most genes associated with A/SP include nucleotide repeat expansions (mostly for hereditary ataxias), single-nucleotide variations, small insertion/deletion events leading to frameshift and/or occurrence of premature stop codon, and large deletions or duplications that affect one or more genes. Ongoing discoveries of genetic abnormalities clearly indicate that disruption of any pathway, organelle functioning, or cellular process can lead to A/SP [1].

Due to this phenotypic and physiopathological heterogeneity, Sanger sequencing of candidate genes or panel approaches often fail to lead to a diagnosis. Next-generation sequencing (NGS), which allows the simultaneous testing of the majority of genes involved in human pathology, may overcome this difficulty. We aimed to evaluate the efficacy of clinical exome-capture sequencing followed by targeted analysis of genes linked to A/SP for the identification of variants in a cohort of 366 consecutive patients with undiagnosed A/SP or related disorders. Establishing the genetic diagnosis in patients is important for disease prognosis and clinical care since few forms of A/SP are treatable, and most are symptomatically managed. While establishing the molecular diagnosis of a large cohort of A/SP patients, we identified many patients with unexpectedly mild clinical presentation with respect to the mutant gene. We discuss the reasons for these discrepancies, which include translation reinitiation, a rarely identified mechanism of hypomorphic presentation.

MATERIALS AND METHODS

Patients and clinical information collection

Between 2015 and 2019, we tested by NGS 366 families referred by 106 distinct clinicians from more than 25 different institutions. These families had previous exclusion of SCA1, -2, -3, and -6, and Friedreich ataxia diagnosis, and of AVED diagnosis based on normal serum vitamin E levels. Some families were previously reported as case reports [6–11] or as small cohorts [12–14]. Genetic analysis was performed after signature of a written informed consent approved by the local ethics committees.

Clinical exome sequencing and data analysis

Clinical exome sequencing was performed using the TruSight One Expanded kit (TSOex, www.illumina.com/trusightone) that targets approximately 6,700 genes, most of them involved in human inherited diseases. Sequencing was performed using Illumina MiSeq or NextSeq technology with 150-bp paired-end reads (Montpellier CHRU NGS platform). Sequence alignment and variant calling were performed following the Broad Institute's Genome Analysis Toolkit (GATK) best practices, using the in-house pipeline Nenufaar (https://github.com/beboche/nenufaar). Sequence reads were aligned against the reference human genome (UCSC hg19). Variants were annotated with Annovar (http://annovar.openbioinformatics.org/) and Variant Studio (www.illumina.com/variantstudio) Copy-number variation (CNVs) analysis was performed with in-house algorithms that compare exon coverage ratios between patients of the same run (as described in Marelli et al. 2016 [13] for MiSeq runs and MobiCNV algorithm for NextSeq runs, https://github.com/Mobidic/MobiCNV). The mean depth of coverage per sample was over 100×, and on average more than 95% of the targeted regions were covered at a minimum level of 30×. In silico filtering was performed on a panel of 490 genes, corresponding to the majority of known ataxia and related disorder genes, using American College of Medical Genetics and Genomics/Association for Molecular Pathology (ACMG/AMP) guidelines for clinical sequence interpretation. The ACMG/AMP classification of the variants was performed using the MobiDetails software [15] (https://github.com/beboche/MobiDetails). Variants with a global population frequency >1% were excluded (gnomAD, 1000 Genomes). Variants with a frequency >0.1% in genes for dominant or X-linked conditions were classified as benign. Pathogenicity arguments were provided by ClinVar (https://www.ncbi.nlm.nih.gov/clinvar) or Clinsig (https://www.ncbi.nlm.nih.gov/clinvar/docs/clinsig) pathogenic match, deleterious prediction by SIFT and/or PolyPhen-2 for missense variants, prediction of splice site alteration or cryptic site activation by NNsplice (https://www.fruitfly.org/seq_tools/splice.html) and MaxENT (http://hollywood.mit.edu/burgelab/maxent/Xmaxentscan_scoreseq_acc.html) softwares, prediction of truncation (nonsense and frameshift variants) or prediction of deleterious in-frame variants (conservation with BLAST searches). In case no pathogenic variant was identified in the in silico 490 gene panel, the entire clinical exome was analyzed with the same guidelines. Familial segregation of probable pathogenic variants, in relation with the patient's presentation, were confirmed by trio analysis or Sanger sequencing.

RESULTS

We established a positive molecular diagnosis for 168 of 366 families analyzed by clinical exome, by identification of clearly or very probably pathogenic variants in the patients (diagnostic yield of 46%). A summary of the clinical presentations as well as of the identified variants is given in the Supplemental Table 1. Among the positive families, the mean age of onset was 19 years and ranged from 1 to 53 years, with 88 index cases (52%) presenting signs during childhood (before 12 years) and 25 additional index cases (15%) with first signs before 25 years. Fifty-five families were multiplex with a suspected recessive or dominant inheritance while the other cases were sporadic. Consanguinity was reported for 22 families. The presence of cerebellar atrophy plus spasticity was correlated with a higher positive yield. Overall, pathogenic variants were found in 83 OMIM genes, including *RORA* that was identified in the course of this study [12], since *RORA* was included in the clinical exome sequencing kit (TSOEx) prior to pathogenic variant identification. Fifty-six families had dominant pathogenic variants in 32 different genes, 109 others had recessively inherited biallelic variants in 50 distinct genes, and 2 had X-linked inheritance (*PLP1* and *PDHA* genes). Dominantly transmitted and X-linked pathogenic variants were confirmed by familial analysis (Fig. 1). In *trans* recessive and de novo pathogenic variants were confirmed by parental analysis (Supplemental Table 1).

Most frequently mutated genes

Among the 83 mutated genes, 15 were responsible for half of the positive cases in our study. The five most frequently mutated genes are *SPG7* (13 families), *SETX* (12 families), *SACS* (10 families), *SYNE1* (9 families), and *PRKCG* (7 families). They account for 30% of the diagnoses. The 10 other frequently mutated genes are *ANO10*, *PLA2G6*, *KIF1A*, *STUB1*, *CACNA1A, SPAST*, *CC2D2A*, *KCNC3*, *CYP7B1*, and *GCH1* and account for 21% of the diagnoses. In the following result section, the disease acronym is given in brackets after the gene acronym.

SPG7 (#SPG7). The p.Ala510Val pathogenic variant, long considered as a polymorphism due to the high frequency in populations of European descent (with an estimated carrier frequency of 1.2%), has been identified in homozygosity or compound heterozygosity in 10 families [16, 17]. All patients with biallelic *SPG7* variants had cerebellar atrophy seen on cerebral magnetic resonance image (MRI) and had spasticity associated with ataxia, with the exception of two families having isolated ataxia. The age of onset of the disease ranged from 15 to 53 years with a mean of 31 years, plus one particular case with onset at 4 years. This very early onset may be explained by comorbidity or by modifier genes. *SETX* (#AOA2/SCAR1). Biallelic *SETX* pathogenic variants were identified in 10 families with ataxia/oculomotor

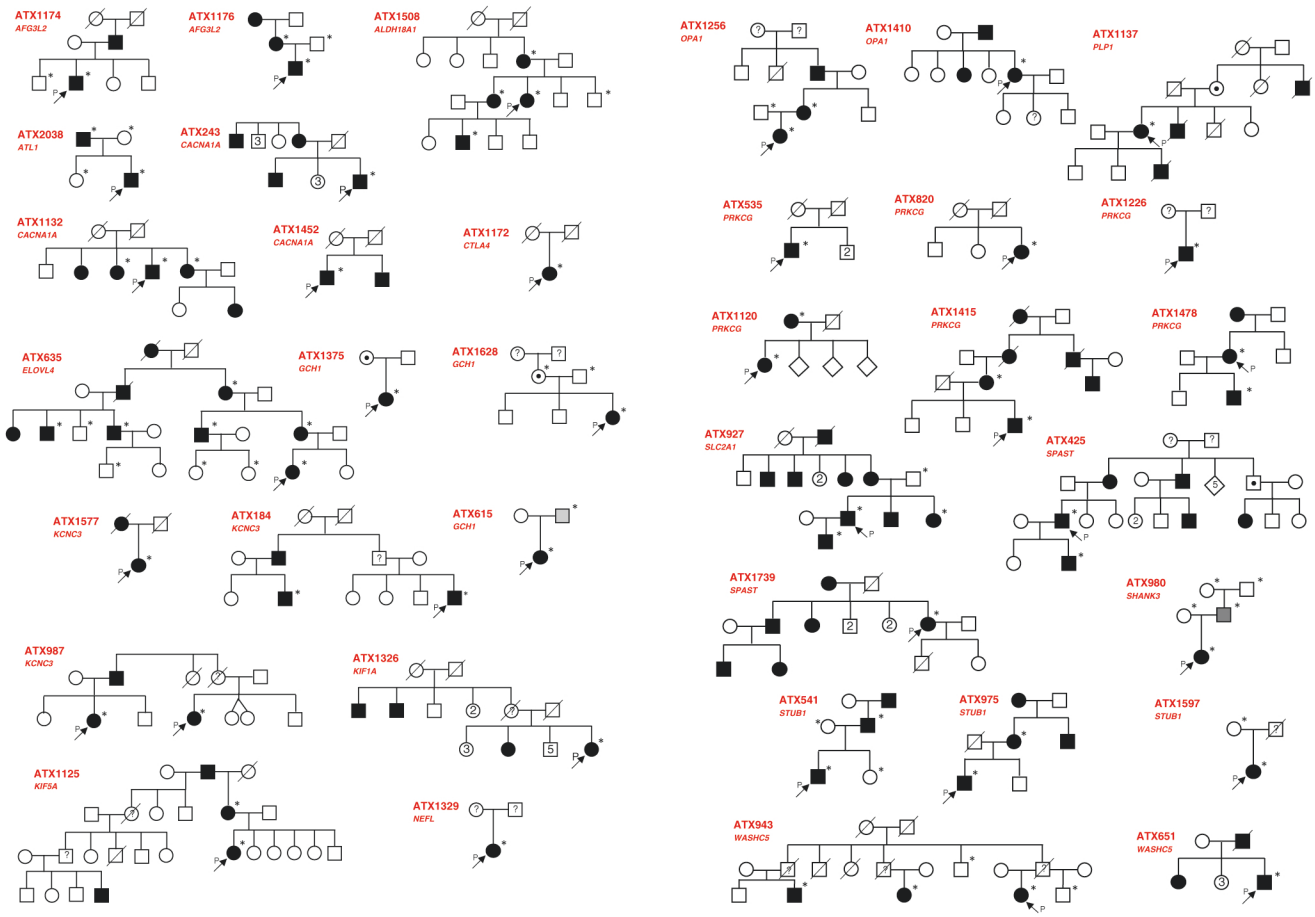

Fig. 1 Familial segregation of dominantly and X-linked inherited pathogenic variants. Families are classified according the alphabetical order of the mutated gene. Index cases are indicated by an arrow. Individuals analyzed for presence or absence of the pathogenic variant are indicated by an asterisk (*): in all cases, affected individuals were heterozygous and healthy individuals tested negative for the variant. Asymptomatic obligate heterozygotes are indicated by a dot within the individual symbol and patients with paucisymptomatic presentation are indicated by a gray symbol. A question mark (?) indicates that the clinical status of the parent is not known.

apraxia type 2 (AOA2) and serum AFP elevation in all cases. Age of onset was ranging from 10 to 20 years. Copy-number variation (CNV) was particularly relevant for this gene, with three families having whole exon deletions and one family with a duplication of exons 5, 6, 7, and 8. Single- or few-nucleotide deletions were identified in five additional families. *SYNE1* (#SCAR8). Age of onset of the 9 patients was generally late, ranging from 8 to 48 years with a mean of 30 years. They presented with isolated ataxia and absence of peripheral neuropathy. Signs of pyramidal irritation were present in only three. All had cerebellar atrophy on MRI. Almost all variants of this gene were high protein impact variants. The only missense variant that we identified (p.Met57Lys) alters a highly conserved amino acid of the calponin-homology (actin-binding) domain of SYNE1. *SACS* (#ARSACS). All patients had onset before 5 years of age, and had ataxia associated peripheral neuropathy at the age of diagnosis. Profound deafness and auditory evoked potential abnormalities were identified in patients from two families, respectively. T2-weighted cerebral MRI showed typical linear hypointensities in the pons for five of six patients for whom detailed MRI report was available. *PRKCG* (#SCA14). Age at onset of our patients ranged from 19 to 39 years, with a mean of 31 years. Most missense variants identified in our patients are located in the C1 (diacyl-glycerol [DAG] binding) domain, and are thus predicted to cause constitutive activation (gain of function) of PRKCG. A single pathogenic variant, p.Leu483Val, was located in the Walker B motif of the kinase domain (proton acceptor site in the ATP hydrolysis reaction), in accordance with published data since very few missense pathogenic variants of the PRKCG kinase domain have been reported to date (p.Asp480Val [18] and p.Phe643Leu [19]).

Pathogenic variants that were difficult to identify or confirm

SHANK3 (#PHMDS). A 6-year-old boy (ATX980) was referred for psychomotor and intellectual retardation, hypotonia, and signs of cerebellar ataxia. Cerebral MRI showed diffuse nonspecific leukopathy. He had a pathogenic nonsense variant, p.Gln106*, in *SHANK3* that led to the diagnosis of Phelan–McDermid syndrome. Surprisingly, the variant was present in the asymptomatic father but turned out to be absent from both paternal grandparents, indicating de novo occurrence in the child's father. Subsequent Sanger sequencing of several peripheral samples of the father revealed somatic mosaicism in only one of two jugal samples (oral brush sampling, Fig. 2), but neither in the 2nd jugal cell sample, nor in hair bulb samples or blood, in accordance with the absence of signs in the father. *SYNE1* (#SCAR8). The index case of family ATX1027 was compound heterozygous for the frameshift pathogenic variant c.18083delT, p.(Leu6028Argfs*23), and the c.4690-9A>G variant. This variant is predicted to create a novel cryptic acceptor splice site (CAG) 8 nucleotides upstream from the wild-type acceptor site of intron 35 (MaxEnt score = 5.36) and to weaken the wild-type splice acceptor site (MaxEnt score decreases from 6.03 to 0.97). Usage of the new cryptic splice site would cause a frameshift and a premature stop codon at position 1601 (p.[Ile1564Valfs*38]). *NFU1* (#MMDS1). A 17-year-old adolescent was referred for childhood-onset paraplegia and spinal cord

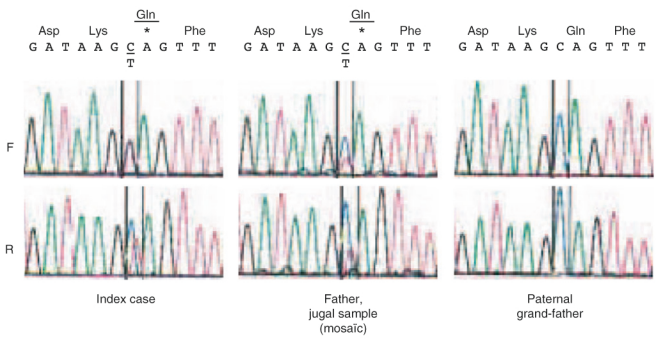

Fig. 2 Sanger sequencing of *SHANK3* exon 3 in family ATX980. F and R indicate sequences obtained with the forward and reverse primers, respectively. Nucleotide sequence and amino acid prediction are indicated on top (*, stop codon). The father is mosaic for the pathogenic variant (c.316C>T, p.Gln106*) he transmitted to his son (index case) only in the right jugal sample (lower mutant signal [T], higher wild-type signal [C]). Paternal left jugal sample, hair bulb and blood sample revealed a sequence profile identical to the one of the index case (not shown). The paternal grandfather has a normal sequence profile (C allele), as has the paternal grandmother (not shown), demonstrating the de novo occurrence of the c.316C>T pathogenic variant in the asymptomatic father.

atrophy (ATX1767). He was heterozygous for a previously reported pathogenic missense variant p.Gly208Cys [20] in *NFU1* that codes for a mitochondrial protein involved in iron–sulfur (Fe–S) cluster synthesis. No other possibly pathogenic exonic variant was identified. We identified a variant, c.62+89G>A, that was located very close to a known very weak cryptic donor splice site, at position c.62+91 (GTGGGT). The variant is predicted to activate the c.62+91 splice site (NNsplice score increases from 0.13 to 0.80), which reaches a score that is higher than the score of the normal splice site at position c.62+1 (NNsplice score of 0.68). Analysis of the parents confirmed that the two variants are biallelic. The transcript that results from the alternative splice site contains an in-frame stop codon at position 22 and encodes a severely truncated protein. The moderate phenotype of the patient is presumably explained by the presence of residual amounts of normal NFU1 protein produced from normally spliced transcripts. *MAN2B1* (#MANSA). We identified in a 44-year-old man presenting with ataxia, intellectual disability, and pancytopenia, a splice pathogenic variant of *MAN2B1* (c.2437-2A>G) associated in *trans* with a previously reported missense change, p.Glu402Lys, classified as benign because it was associated in *cis* with another pathogenic variant (c.1026+2T>G) [21]. Retrospective biochemical exploration of alpha-mannosidase activity (0.22 µkat/kg prot.; normal range: 14-66 µkat/kg prot.) confirmed the diagnosis of MANSA, and therefore allowed to reclassify the missense change p.Glu402Lys, which was not associated in *cis* with the c.1026+2T>G change in our patient, as likely pathogenic.

Unusual mechanisms for mild clinical presentation

We identified many patients with a clinical presentation milder than the expected associated presentation for the mutant gene. We identified a mild presentation in at least 35 of the diagnosed families (Table 1), 31 of which are in recessive or X-linked families (clinically highly variable *SPG7* families were not included). In most cases, the milder presentation was explained by a presumably mild missense pathogenic variant (for example affecting a moderately conserved amino acid position) or a weak splice site variant outside from the canonical -1 and -2 acceptor and +1 and +2 donor splice site positions (such as the one discussed above). In a few cases, we identified pathogenic variant that are predicted to be severely disruptive (i.e., nonsense or frameshift variants) but in patients with an unusually mild presentation. In the five families presented below, we suspect that the mild clinical presentation of the patients despite prediction of a severe protein disruption might be explained by either of two mechanisms: (1) truncation of a C-terminal, less important, part of the protein; (2) reinitiation of translation. A short case report for each of the five families is given in the Supplemental data.

Truncating pathogenic variant leading to mild impairment

CEP290 (#JBTS5). We identified the homozygous frameshift pathogenic variant c.7366_7369delTTAA (p.[Thr2457Alafs*27]) in the *CEP290* Joubert syndrome gene of a patient (ATX36) with congenital retinitis pigmentosa, onset of ataxia during teenage, and absence of molar tooth sign (only isolated vermian atrophy was present on MRI). The mild phenotype of our patient might be explained by the replacement of only the last 22 amino acids of the CEP290 protein (of 2,478) by 26 amino acids coded by the frameshifted sequence. Moreover, because the pathogenic variant is located in the last exon of *CEP290*, the corresponding transcript is not expected to undergo nonsense mediated RNA decay (NMD). *NDUFAF2* (#MC1DN10). The homozygous nonsense pathogenic variant p.Trp74* was identified in the *NDUFAF2* gene of a 37-year-old patient (ATX787) with onset of progressive bilateral visual loss (optic neuropathy) in early childhood and ataxia in adolescence with moderate disease progression and absence of cerebellar atrophy (Fig. 3a). No muscle biopsy was available for studies of the mitochondrial respiratory chain. The *NDUFAF2* protein is very small (169 amino acids) and the conserved domain (NDUFA12-like domain, Fig. 4) is located in the N-terminal part, from amino acid positions 23 to 84. This domain is conserved in most eukaryotes (Fig. 4). The nonsense pathogenic variant at position 74 might thus allow the synthesis of a truncated but possibly partially functional protein, unlike the *NDUFAF2* truncating variants associated with short survival (7 months to 13 years), which are located at the beginning of the NDUFA12-like domain [22, 23]. *PEX11b* (#PBD14B). The homozygous frameshift pathogenic variant c.630_631insAGAA (p.[Val211Argfs*8]) was identified in the *PEX11b* gene of two brothers (family ATX608) with developmental and cognitive delay, dysmorphia, congenital cataract, and deafness. Cerebellar ataxia appeared at age 35 years and both brothers remained autonomous until the age of 55 years. Cerebral MRI showed mild cerebellar and cerebral atrophy (Fig. 3b, c). Retrospective study of peroxisomal biomarkers revealed only a slight decrease of erythrocytic plasmalogen (DMA/DME (C16:0) ratio: 0.053, normal range: 0.068–0.085; DMA/DME (C18:0) ratio: 0.121, normal range: 0.152–0.182) and a VLCFA ratio just above the upper limit of normal range (C26:0/C22:0 at 0.020, normal values < 0.019). Pristanic and phytanic acids levels were normal (Supplemental Table 2). The later age at onset of the neurological signs of the two brothers, compared to the only *PEX11b* neurologic case reported to date (with the homozygous nonsense pathogenic variant p.Glu22* [24]) might be explained by the distal position of the frameshift pathogenic variant (codon 211 of 259 total), past the highly conserved domain of PEX11b, also conserved in most eukaryotes (Fig. 4).

Translation reinitiation

PEX10 (#PBD6B). We identified *PEX10* compound heterozygous frameshift pathogenic variants in a 31-year-old patient (ATX1177) who showed the first signs of cerebellar ataxia with cerebellopontine atrophy (Fig. 3d), cerebellar hyperintensities (Fig. 3e), deafness, and scoliosis at the age of 20 years. There was neither pyramidal involvement nor peripheral neuropathy. Retrospective peroxisomal investigations showed moderately elevated serum VLCFA (C26:0 at 1.7 micromol/L, normal values < 1.32 micromol/L) while phytanic acid, C22:0, and C24:0 levels were normal (Supplemental Table 2). The compound heterozygous c.26dupC and c.874_875delCT pathogenic variants, which are predicted to

Table 1. Hypomorphic pathogenic variants of patients with a mild clinical presentation.

ATX number	Gene	Nucleotide change	Amino acid change	Status	Classical phenotype	Patient's phenotype	Mechanism of hypomorphism
ATX1362	*ACO2*	c.220C>G	p.Leu74Val	het	Encephalopathy with optic atrophy	Isolated optic atrophy	Mild missense pathogenic variant
		c.2048G>A	p.Gly683Asp	het			
ATX1007	*ACO2*	c.940+5G>C	splicing	het	Encephalopathy with optic atrophy	Spastic paraplegia/ataxia/optic atrophy	Partially altered splicing
		c.2135C>T	p.Pro712Leu				-
ATX498	*NPC1*	c.1156A>G	p.Ser386Gly	het	Onset is usually in childhood	Disease onset at 30 years	Mild missense pathogenic variant
		c.1892T>G	p.Met631Arg				
ATX42	*NPC1*	c.352_353delAG	p.Gln119Valfs*8	het	Onset is usually in childhood	Pure cerebellar ataxia/onset at 12 and 20 years (siblings)	-
		c.57+4A>G	splicing				Partially altered splicing
ATX1200	*C19ORF12*	c.187G>C	p.Ala63Pro	hom	Neurodegeneration with brain iron accumulation/onset in infancy	Isolated spastic paraplegia/onset at 11 years	Mild missense pathogenic variant
ATX787	*NDUFAF2*	c.221G>A	p.Trp74*	hom	Leukoencephalopathy/onset in infancy/ early death reported	Onset in childhood/normal cMRI/ present age 37 years	Truncation of the nonconserved C-terminal domain
ATX1767	*NFU1*	c.622G>T	p.Gly208Cys	het	Multiple mitochondrial dysfunction syndrome/onset at birth/death by age 15 months	Spastic paraplegia/onset in childhood/present age 17 years	-
		c.62+89G>A	splicing				Partially altered splicing
ATX286	*ATM*	c.3712_3716del TTTTA	p.Leu1238Lysfs*6	het	Ataxia telangectasia/onset before 5 years	Onset of ataxia at 24 years	-
		c.7271T>G	p.Val2424Gly				Mild missense pathogenic variant
ATX1177	*PEX10*	c.26dupC	p.Glu9Glyfs*41	het	Encephalopathy/onset in infancy or early childhood	Cerebellar ataxia/onset at 20 years	Translation reinitiation
		c.874_875delCT	p.Leu292Valfs*66				
ATX608	*PEX11B*	c.630_631insAGAA	p.Val211Argfs*8	hom	Onset of ataxia at 12 years/severe neuropathy	Cerebellar ataxia/onset at 35 years	Truncation of the less conserved C-terminal domain
ATX1219	*POLR3A*	c.1771-7C>G	splicing	het	Leukoencephalopathy/onset in infancy/ early death reported	Isolated spastic ataxia/onset at 6 years/present age 45 years	Partially altered splicing
		c.2563C>T	p.Arg855Trp				-
ATX36	*CEP290*	c.7366_7369del TTAA	p.Thr2457Alafs*27	hom	Joubert or Joubert-like syndrome	Ataxia with retinitis pigmentosa/ onset of ataxia at 12 years	Frameshift at the very end of the protein
ATX910	*FASTKD2*	c.535delT	p.Pro180Leufs*27	hom	Leukoencephalopathy/onset in infancy/ early death reported	Isolated spastic ataxia/onset at 42 years/present age 51 years	Translation reinitiation
ATX94	*PEX6*	c.1802G>A	p.Arg601Gln	het	Encephalopathy/onset in infancy or early childhood	Late onset ataxia	Mild missense pathogenic variant
		c.2308G>T	p.Gly770Trp	het			
ATX1712	*STUB1*	c.433A>G	p.Lys145Gln	het	Progressive ataxia with axonal neuropathy/onset in second decade	Late onset cerebellar ataxia without axonal neuropathy	Mild missense pathogenic variant
		c.518G>A	p.Arg173His	het			

Table 1 continued

ATX number	Gene	Nucleotide change	Amino acid change	Status	Classical phenotype	Patient's phenotype	Mechanism of hypomorphism
ATX107	*HSD17*	c.817C>T	p.Arg273Cys	het	Perrault syndrome including neurologic impairment, hypogonadism and psychomotor delay	Spastic ataxia without hypogonadism or psychomotor delay	Mild missense pathogenic variant
		c.1207G>A	p.Gly403Arg				
ATX412	*ERCC4*	c.2395C>T	p.Arg799Trp	hom	Xeroderma pigmentosum/variable severity of neurological impairment/early death reported	No xeroderma pigmentosum/ onset at 30 years/present age 72 years	Mild missense pathogenic variant
ATX364	*ERCC4*	c.578_583del GGCCAA	p.Pro194_ Arg195del	het	Xeroderma pigmentosum/variable severity of neurological impairment/early death reported	No xeroderma pigmentosum/ onset at 30 years	-
		c.2395C>T	p.Arg799Trp				Mild missense pathogenic variant
ATX1137	*PLP1*	c.21delT	p.Cys7Trp*6	het	Spastic paraparesis	Mild neurological impairment	Lyonization
ATX1395	*INPP5E*	c.922A>G	p.Met308Val	het	Joubert syndrome/congenital/molar tooth sign	No molar tooth sign/onset of ataxia at 1 year	Mild missense pathogenic variant
		c.1456C>T	p.Arg486Cys				-
ATX469	*PMM2*	c.323C>T	p.Ala108Val	Het	High lethality in the first year of life/ severe neurologic impairment	Mild neurological impairment/ present age 72 years	Mild missense pathogenic variant
		c.620T>C	p.Phe207Ser				-
ATX1383	*PDHA1*	c.483C>T	splicing (ESE)	het	Onset in early childhood/severe neurological impairment	Late onset (12 years)/mild neurological impairment	Partially altered splicing and Lyonization
ATX635	*ELOVL4*	c.698C>T	p.Thr233Met	het	Cerebellar ataxia/onset in young adulthood	Ataxia with onset ranging from 18 to 40 years	Mild missense pathogenic variant
ATX536	*CYP27A1*	c.193C>T	p.Gln65*	het	Tendon xanthomas/neuropathy/ cerebellar atrophy/onset in teenage years	No xanthomas/no neuropathy/no cerebellar atrophy/ataxia onset at 30 years	-
		c.1183C>T	p.Arg395Cys				Mild missense pathogenic variant
ATX1332	*ANO10*	c.220G>C	p.Ala74Pro	het	Pure cerebellar ataxia/onset in teenage or young adulthood	Late onset cerebellar ataxia (50 years)	Mild missense pathogenic variant
		c.512T>C	p.Phe171Ser				-
ATX1026	*KCNJ10*	c.626T>C	p.Ile209Thr	hom	Sensorineural deafness/electrolyte imbalance	No electrolyte imbalance/no deafness	Mild missense pathogenic variant
ATX1529	*MAN2B1*	c.2437-2A>G	splicing	het	Severe neurological impairment/onset in early childhood	Mild neurological impairment/ onset in teenage	-
		c.1204G>A	p.Glu402Lys				Mild missense pathogenic variant
ATX1537	*XPA*	c.619C>T	p.Arg207*	het	Skin photosensitivity/early onset skin cancer	No skin phenotype/present age 36 years	-
		c.731A>G	p.His244Arg				Mild missense pathogenic variant
ATX940	*ATP8A2*	c.1762C>T	p.Arg588Trp	hom	Psychomotor delay/severe neurological impairment	Mild neurological impairment	Mild missense pathogenic variant
ATX1326	*KIF1A*	c.961G>A	p.Gly321Ser	het	Spastic paraplegia/onset in first or second decade/axonal neuropathy/ cerebellar atrophy	Pure adult onset spastic paraplegia	Mild missense pathogenic variant

Table 1 continued

ATX number	Gene	Nucleotide change	Amino acid change	Status	Classical phenotype	Patient's phenotype	Mechanism of hypomorphism
ATX1452	*CACNA1A*	c.2158G>C	p.Ala720Pro	het	Episodic ataxia/onset in childhood or adolescence	Late onset ataxia (51 years)	Mild missense pathogenic variant
ATX1172	*CTLA4*	c.151C>T	p.Arg51*	het	Severe early onset impairment	Late onset neurological impairment	Incomplete penetrance
ATX1170	*TTC19*	c.626T>C	p.Leu209Pro	hom	Neurological impairment/onset in early adulthood	Very late onset ataxia (50 years)/no spasticity	Mild missense pathogenic variant
ATX681	*PNPLA6*	c.3322C>T c.4075C>T	p.Arg1108Trp p.Arg1359Trp	het	Onset of ataxia in the first decade/ sensorimotor axonal neuropathy	Late onset ataxia (30 years)/\no spasticity/no neuropathy	Mild missense pathogenic variant
ATX1202	*AP5Z1*	c.59A>T c.1034G>A	p.Glu20Val p.Arg345Gln	het	Spastic ataxia	Isolated ataxia/no spasticity	- Mild missense pathogenic variant

Fig. 3 Cerebral and spinal cord magnetic resonance image (MRI) of selected patients. Patient ATX787 with the homozygous *NDUFAF2* pathogenic variant: median sagittal T2-STIR-weighted brain and spinal cord section, revealing spinal hyperintensities (**a**), also seen on axial cervical spinal cord section (inset). Patient ATX608 with the homozygous *PEX11b* pathogenic variant: axial T2 FLAIR-weighted cerebral section revealing occipital cortical atrophy (**b**) and axial T2 FLAIR-weighted cerebellar section showing very mild cerebellar atrophy (**c**). Patient ATX1177 with *PEX10* pathogenic variants: median sagittal T2 FLAIR-weighted cerebral section revealing pronounced cerebellar atrophy (**d**) and axial T2 FLAIR-weighted cerebellar section showing hemispheric cerebellar hyperintensities (**e**). Patient ATX910 with the homozygous *FASTKD2* pathogenic variant: axial T2 FLAIR-weighted cerebral section: normal imaging (**f**) and median sagittal T2 FLAIR-weighted cerebral section showing moderate cerebellar atrophy (**g**).

cause a frameshift with a premature stop codon (p.[Glu10Glyfs*41] and p.[Leu292Valfs*66], respectively), appear inconsistent with the patient's mild impairment. The mild phenotype might be explained by translation reinitiation on the c.26dupC allele at the downstream methionine 145. This would allow the synthesis of the most conserved part of the PEX10 protein, including the RING finger zinc-binding domain (Fig. 4). *FASTKD2* (#COXPD44). Similarly, translation reinitiation might also be involved for the patient of family ATX910, who is homozygous for the c.535delT pathogenic variant, located in exon 1, and predicted to cause the frameshift change p.(Pro180Leufs*27) in *FASTKD2*. The patient had cerebellar ataxia beginning at age 42 years, associated with mild spastic paraplegia, nystagmus, and transient myoclonus. Scale for the assessment and rating of ataxia (SARA) score when she was 50 years old was 12/40. Cerebral and spinal cord MRI did not reveal marked abnormalities besides mild, generalized atrophy of brain and cerebellum (Fig. 3f, g). Electroneuromyography was normal. Retrospective muscle biopsy analysis showed moderate mitochondrial complex I and IV deficiency (cytochrome C oxidase, C [IV]: 56.6 nmoles/min/kg prot., normal values ≥64.5 nmoles/min/mg; NADH-ubiquinone reductase, C[I]: 9.1 mmoles/min/kg prot., normal values ≥9.3 mmoles/min/kg prot.; Supplemental Table 3). The very mild clinical presentation of our patient might be explained by translation reinitiation at methionine 188, which is immediately downstream of the frameshift. The first 259 amino acids of the FASTKD2 protein are encoded by exon 1 and define a very poorly conserved part of the protein (Fig. 3). Reinitiation at methionine 188 would allow synthesis of the FAST_1, FAST_2, and RAP domains (Fig. 4), which might be sufficient for partial functionality of the N-terminally truncated protein.

DISCUSSION

We identified by clinical exome sequencing the molecular cause for 168 families with neurodegenerative disorders including ataxia, spastic paraplegia, and inherited movement disorders, of

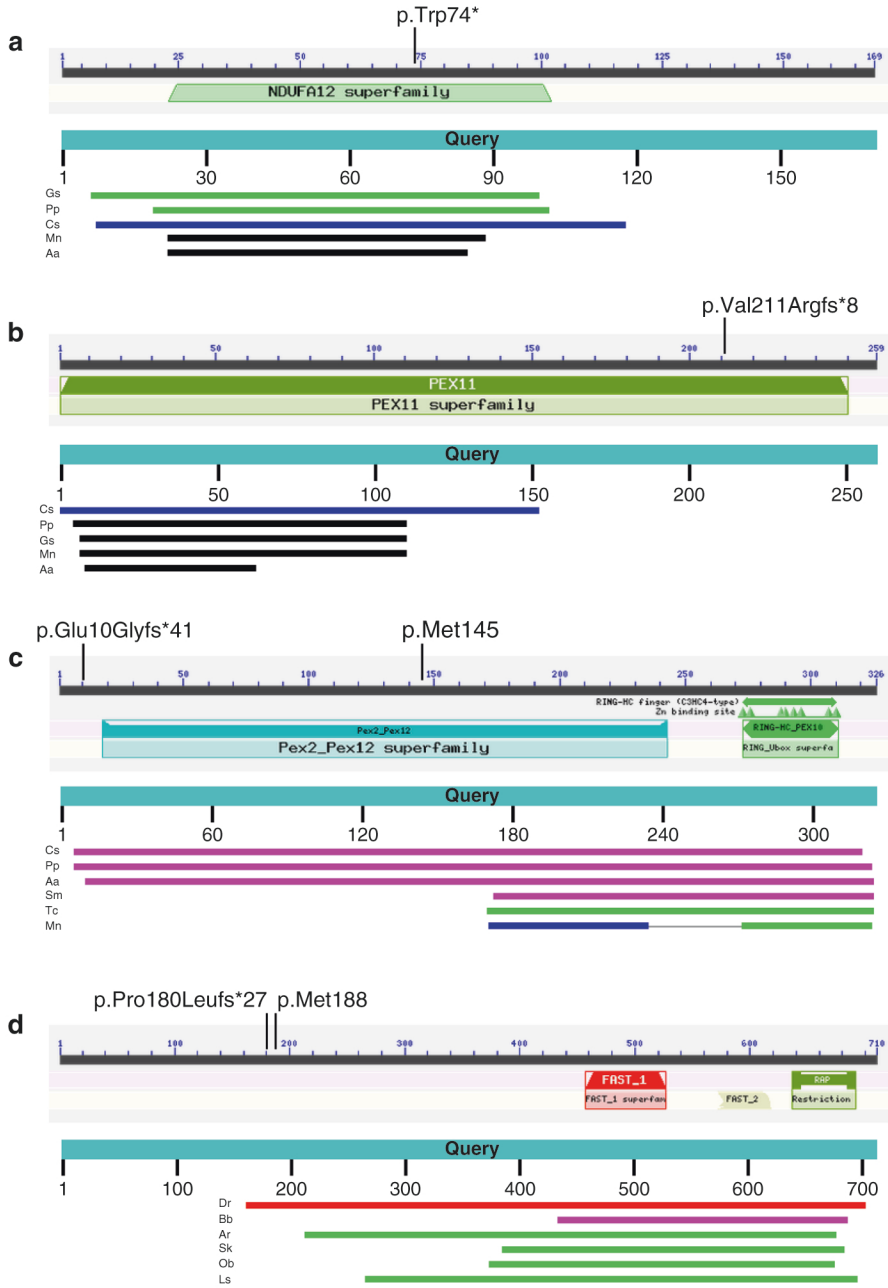

Fig. 4 Domain conservation of selected proteins. Known functional domains are indicated below the scale bar. Position of the truncating pathogenic variant and of the putative reinitiating methionine are indicated above the scale bar. Extent of conservation in selected distant species is indicated below the Query bar (protein BLAST search, National Center for Biotechnology Information, US National Library of Medicine). Selected species: Cs *Coccomyxa subellipsoidea*, Gs *Galdieria sulphuraria*, Pp *Physcomitrella patents*, Mn *Monoraphidium neglectum* (plants), Aa *Aphanomyces astaci*, Sm *Symbiodinium microadriaticum*, Tc *Trypanosoma cruzi* (protists), Ar *Asterias rubens*, Bb *Branchiostoma belcheri*, Dr *Danio rerio* (vertebrate), Ls *Leptidea sinapis*, Ob *Octopus bimaculoides*, Sk *Saccoglossus kowalevskii* (invertebrates). The putative truncated protein products cover the conserved domains, suggesting partial functionality. (**a**) NDUFAF2, (**b**) PEX11b, (**c**) PEX10, (**d**) FASTKD2. Since FASTKD2 is significantly less conserved, closer species (invertebrates and one distant vertebrate, zebra fish) were used for protein BLAST search.

366 families tested. We report the clinical and molecular characterization of the patients from these 168 families. Our results confirm the frequent involvement of the *SPG7*, *SACS*, *SETX*, and *SYNE1* genes in ataxia cases, in agreement with recent studies [25]. The diagnostic yield (46%) therefore compares very favorably even with studies based on entire exome sequencing [25–28] since we have not retained as potential positive diagnoses the cases with a single heterozygous recessive pathogenic variant despite good clinical correlation. The availability of biochemical markers or functional studies carried out for variants of difficult interpretation made it possible to retrospectively confirm several diagnoses. The occurrence of de novo pathogenic variant was confirmed in 17 families, and is suspected in 4 others. In the case of the *SHANK3* variant, the asymptomatic father was mosaic for the de novo pathogenic variant. We confirm the existence congenital spinocerebellar ataxia with neurodevelopmental delay due de novo pathogenic variant in *CACNA1G* [29] and in the N-terminal calponin-homology domain and the second spectrin repeat domain of *SPTBN2*, while initial *CACNA1G* cases had dominantly inherited adult onset spinocerebellar ataxia (SCA42 [30]) and initial

SPTBN2 cases had dominantly inherited adult onset spinocerebellar ataxia (SCA5 [31]) or recessive congenital ataxia (SCAR14 [32]).

We also confirm the particular presentation recently identified for the *STUB1* and *POLR3A* genes. We identified three families with dominant spinocerebellar ataxia and cognitive–affective syndrome (SCA48 [33]) due to *STUB1* missense pathogenic variants and one family with late onset (40 years) autosomal recessive *STUB1* ataxia (SCAR16 [14]). The two sisters with a diagnosis of SCAR16 were compound heterozygous for the p.Arg173His and p.Lys145Gln pathogenic variants, the mild presentation being presumably due the p.Lys145Gln variant, not predicted as pathogenic by the SIFT (score = 0.28) and PolyPhen-2 (score = 0.445) programs, but previously reported in two siblings with onset at 30 years [34]. Initial SCAR16 cases had onset usually in the second decade [35]. We also identified slowly progressive ataxia and spasticity (ambulation without assistance at the age of 45 years) in a patient who is compound heterozygous for two *POLR3A* pathogenic variants, including the reported hypomorphic splice variant c.1771-7C>G [36]. Classical *POLR3A* presentations include Wiedemann–Rautenstrauch syndrome (WRS) or hypomyelinating leukodystrophy (4H syndrome) [37].

As exemplified in the *NFU1*, *STUB1*, and *POLR3A* cases, ataxia and/or spastic paraplegia was accounted in an important fraction of cases by hypomorphic pathogenic variants in genes that would otherwise cause severe syndromes when mutated. A mild presentation accounted for at least 20% of all diagnosed families, and for 28% of the recessive and X-linked families (31/110). In all cases, the hypomorphic variants impacted the canonical (MANE Select) transcript. In silico prediction of these hypomorphic/partial loss-of-function variants often represents a significant diagnostic challenge. We were able to distinguish four types of mechanism of partial loss of function: (1) semiconservative missense changes at moderately conserved amino acid positions, (2) moderate alteration of splicing by variant of noncanonical positions and/or creation of cryptic splice sites, (3) C-terminal truncations that remove small or less conserved parts of the protein, (4) reinitiation of translation after an early truncation variant, resulting in N-terminal truncation (Table 1). Hypomorphic C- and N-terminal truncations (mechanisms 3 and 4) are seldom mentioned mechanisms that deserve further discussion with our *CEP290*, *NDUFAF2*, *PEX11b*, *PEX10*, and *FASTKD2* examples.

The C-terminal frameshift of *CEP290*, p.(Thr2457Alafs*27), replaces less than 1% of the protein by a frameshifted sequence of roughly similar length, resulting in only congenital retinitis pigmentosa and teenage onset ataxia. The same p.(Thr2457Alafs*27) pathogenic variant, c.7366_7369delTTAA, was previously reported in a patient with Joubert syndrome and retinitis of pigmentosa but without additional details [38] while other *CEP290* truncating pathogenic variants result in either Joubert type 5, Meckel, Bardet–Biedl, Senior–Loken type 6, and cerebello–oculo–renal syndromes [39]. The *PEX11b* and *NDUFAF2* C-terminal truncating pathogenic variants are strikingly different, as they remove over one fifth to one half, respectively, of remarkably small proteins. Our conservation analysis of PEX11b and NDUFAF2 sequences in very distant eukaryotic species (plants and protists, Fig. 4) indicate that most of the highly conserved domains are maintained in the truncated proteins. Hence residual activity of the truncated products provides a plausible explanation for the mild presentation of the patients. Indeed, the only previously reported patient with *PEX11b* variant and neurologic impairment had a homozygous proximal nonsense pathogenic variant c.64C>T (p.Glu22*) and presented in childhood with a picture similar to the one of our patients, including moderate mental retardation, congenital cataract, and deafness at the age of 7 years [24]. However, unlike our patients, his neurological impairment began at the age of 12 years with gait disturbances and severe sensory–motor neuropathy requiring him to use a wheelchair for long distances. The later age at onset of the cerebellar ataxia (35 years) and autonomous ambulation until the age of 55 years of our two patients might therefore be explained by the p.Val211Argfs*8 C-terminal truncating pathogenic variant. Likewise, all previously reported patients with *NDUFA*F2 complete loss-of-function variants had proximal nonsense or frameshift pathogenic variants (occurring at amino acid positions 3, 35, 38, and 45) and presented with Leigh syndrome and survival ranging from 7 months to 13 years [22, 23], while our patient with the homozygous p.Trp74* nonsense pathogenic variant is still alive at age 37 years. Residual activity of the C-terminally truncated NDUFAF2 protein appears to be the only explanation for this longer longevity.

Proximal, N-terminal, truncations appear less likely to explain mild presentation. However, reinitiation of protein translation by the use of a methionine downstream of the stop codon was already hypothesized for the initiating methionine variant of *PEX10* (c.2T>C [40, 41]). In both cases, patients were adults with moderate ataxia and onset ranging from 6 to 15 years, at departure from the classical Zellweger syndrome presentation associated with complete loss-of-function variants. A similar mechanism may explain the late onset (20 years) ataxic presentation of our patient with two biallelic *PEX10* frameshift variants, one of which, p.(Glu9Glyfs*41), is located upstream of the putative reinitiating methionine at position 145. In all cases of moderate ataxia with *PEX10* pathogenic variants, the biological values of peroxisomal function were either at the upper limit of the normal range or very slightly increased [41]. Translational reinitiation at methionine 145 would allow the synthesis of the most conserved part of the N-terminal domain and of the highly conserved RING zinc finger domain which is crucial for the functioning of PEX10 protein. Interestingly, a minor *PEX10* transcript (NM_001374426.1, UCSC genome database) that uses an alternative promoter and exon 1 encodes a N-terminally truncated protein that starts at methionine position 145 due to the absence of ATG codon in the alternative first exon, supporting the views that ATG 145 is indeed used for translation initiation and that a short PEX10 protein truncated for the first 144 residues might have some physiological relevance. Similarly, translation reinitiation may also explain the late onset (42 years) cerebellar ataxia of our patient with the homozygous N-terminal frameshift pathogenic variant, p.(Pro180Leufs*27), in *FASTKD2*. Recently, another patient with mild ataxic presentation, late onset, and compound heterozygosity for two pathogenic *FASTKD2* variants including the nonsense variant p.Arg205* was reported [42]. Classical patients with biallelic *FASTKD2* variants have severe, early, epileptic encephalopathy; generalized cerebral atrophy; cardiopulmonary and muscular involvement; and more distal truncating pathogenic variants: p.Arg432* (p.Arg416* in Ghezzi et al. [43]), p.Leu270fs*, p.Arg290*, and p.Ser621fs* [44]. Moreover, the decreased complex IV activity was less pronounced in our patient, compared to the patients with the p.Arg432* pathogenic variant (56% of residual activity against 21%, respectively), consistent with the more severe involvement of the latter. The difference between the mild and severe *FASTKD2* cases might therefore be explained by translation reinitiation at methionine positions 188 and 207, in our and the 2017 reported cases [42], respectively, allowing the synthesis of an N-terminally truncated *FASTKD2* protein with retained FAST_1, FAST_2 domains, and the RNA binding RAP C-terminal domain [45]. Recurrence of potentially hypomorphic N-terminal truncation on both *PEX10* and *FASTKD2* suggests that only a small fraction of genes may undergo synthesis of partially functional proteins through internal translation reinitiation.

In conclusion, we demonstrate that an important fraction of ataxia and/or spastic paraplegia cases are accounted by hypomorphic pathogenic variants, and suggest that N- and C-terminal truncation may account for the partial loss-of-function mechanism in some of the cases. Identification of causative pathogenic variants in 83 different genes, involved in very diverse cellular

mechanisms and metabolic pathways, supports the view that there is no specific mechanism that leads, when disrupted, to ataxia or spastic paraplegia. Rather, partial loss of function in any ubiquitous cellular pathway may lead to ataxia or spastic paraplegia due to the exquisite sensitivity of cerebellar and spinal cord neurons to even mild metabolic insults [1].

DATA AVAILABILITY

Readers can freely access all software used for this study by following the most recent version links mentioned in "Materials and methods." Patients' data are not available on an open-source access database due the large number of hospital centers involved in this study. Data can be made available upon request.

REFERENCES

1. Anheim M, Tranchant C, Koenig M. The autosomal recessive cerebellar ataxias. N Engl J Med. 2012;366:636–646. https://doi.org/10.1056/NEJMra1006610.
2. Synofzik M, Németh AH. Recessive ataxias. Handb Clin Neurol. 2018;155:73–89. https://doi.org/10.1016/B978-0-444-64189-2.00005-6.
3. Sullivan R, Yau WY, O'Connor E, Houlden H. Spinocerebellar ataxia: an update. J Neurol. 2019;266:533–544. https://doi.org/10.1007/s00415-018-9076-4.
4. Marras C, et al. Nomenclature of genetic movement disorders: Recommendations of the international Parkinson and movement disorder society task force. Mov Disord. 2016;31:436–457. https://doi.org/10.1002/mds.26527.
5. Rossi M, et al. The genetic nomenclature of recessive cerebellar ataxias. Mov Disord. 2018;33:1056–1076. https://doi.org/10.1002/mds.27415.
6. Ayrignac X, et al. Two neurologic facets of CTLA4-related haploinsufficiency. Neurol Neuroimmunol neuroinflammation. 2020;7:1–6. https://doi.org/10.1212/NXI.0000000000000751.
7. Marelli C, et al. Plasma oxysterols: Biomarkers for diagnosis and treatment in spastic paraplegia type 5. Brain. 2018;141:72–84. https://doi.org/10.1093/brain/awx297.
8. Guissart C, et al. ATP8A2-related disorders as recessive cerebellar ataxia. J Neurol. 2020;267:203–213. https://doi.org/10.1007/s00415-019-09579-4.
9. Marelli C, Hamel C, Quiles M, Carlander B. ACO2 mutations: A novel phenotype associating severe optic atrophy and spastic paraplegia. Neurol Genet. 2018;0:2–5. https://doi.org/10.1212/NXG.0000000000000225.
10. Roubertie A, et al. AP4 deficiency: a novel form of neurodegeneration with brain iron accumulation? Neurol Genet. 2018;4:1–6. https://doi.org/10.1212/NXG.0000000000000217.
11. Marelli C, et al. Autosomal dominant SPG9: intrafamilial variability and onset during pregnancy. Neurol Sci. 2020;41(Jul):1931–1933. https://doi.org/10.1007/s10072-020-04341-5.
12. Guissart C, et al. Dual molecular effects of dominant RORA mutations cause two variants of syndromic intellectual disability with either autism or cerebellar ataxia. Am J Hum Genet. 2018;102:744–759. https://doi.org/10.1016/j.ajhg.2018.02.021.
13. Marelli C, et al. Mini-exome coupled to read-depth based copy number variation analysis in patients with inherited ataxias. Hum Mutat. 2016;37:1340–1353. https://doi.org/10.1002/humu.23063.
14. Ravel J-M, Benkirane M, Calmels N, Marelli C, Ory-Magne F, Ewenczyk C. Expanding the clinical spectrum of STIP1 homology and U-box containing protein 1-associated ataxia. J Neurol. (in press).
15. Baux D, Van Goethem C, Ardouin O, Guignard T, Roux MKA. MobiDetails: online DNA variants interpretation. Eur J Hum Genet. 2020. https://doi.org/10.1038/s41431-020-00755-z.
16. Klebe S, et al. Spastic paraplegia gene 7 in patients with spasticity and/or optic neuropathy. Brain. 2012;135:2980–2993. https://doi.org/10.1093/brain/aws240.
17. Sánchez-Ferrero E, et al. SPG7 mutational screening in spastic paraplegia patients supports a dominant effect for some mutations and a pathogenic role for p.A510V. Clin Genet. 2013;83:257–262. https://doi.org/10.1111/j.1399-0004.2012.01896.x.
18. Najmabadi H, et al. Deep sequencing reveals 50 novel genes for recessive cognitive disorders. Nature. 2011;478:57–63. https://doi.org/10.1038/nature10423.
19. Stevanin G. Mutation in the catalytic domain of protein kinase. Arch Neurol. 2004;61:1242–1248.
20. Navarro-Sastre A, et al. A fatal mitochondrial disease is associated with defective NFU1 function in the maturation of a subset of mitochondrial Fe–S proteins. Am J Hum Genet. 2011;89:656–667. https://doi.org/10.1016/j.ajhg.2011.10.005.
21. Berg T, et al. Spectrum of mutations in a -mannosidosis. Am. J. Hum Genet. 1999;64:77–88.
22. Ogilvie I, Kennaway NG, Shoubridge EA. A molecular chaperone for mitochondrial complex I assembly is mutated in a progressive encephalopathy. J Clin Invest. 2005;115:2784–2792. https://doi.org/10.1172/JCI26020.
23. Hoefs SJ, et al. Baculovirus complementation restores a novel NDUFAF2 mutation causing complex I deficiency. Hum Mutat. 2009;30:728–736. https://doi.org/10.1002/humu.21037.
24. Ebberink MS, et al. A novel defect of peroxisome division due to a homozygous nonsense mutation in the PEX11β gene. J Med Genet. 2012;49:307–313. https://doi.org/10.1136/jmedgenet-2012-100778.
25. Coutelier M, et al. Efficacy of exome-targeted capture sequencing to detect mutations in known cerebellar ataxia genes. JAMA Neurol. 2018;75:591–599. https://doi.org/10.1001/jamaneurol.2017.5121.
26. Sun M, et al. Targeted exome analysis identifies the genetic basis of disease in over 50% of patients with a wide range of ataxia-related phenotypes. Genet Med. 2019;21:195–206. https://doi.org/10.1038/s41436-018-0007-7.
27. Fogel BL, et al. Exome sequencing in the clinical diagnosis of sporadic or familial cerebellar ataxia. JAMA Neurol. 2014;71:1237–1246. https://doi.org/10.1001/jamaneurol.2014.1944.
28. Ngo KJ, et al. A diagnostic ceiling for exome sequencing in cerebellar ataxia and related neurological disorders. Hum Mutat. 2020;41:487–501. https://doi.org/10.1002/humu.23946.
29. Chemin J, et al. De novo mutation screening in childhood-onset cerebellar atrophy identifies gain-of-function mutations in the CACNA1G calcium channel gene. Brain. 2018;141:1998–2013. https://doi.org/10.1093/brain/awy145.
30. Coutelier M, et al. A recurrent mutation in CACNA1G alters Cav3.1 T-type calcium-channel conduction and causes autosomal-dominant cerebellar ataxia. Am J Hum Genet. 2015;97:726–737. https://doi.org/10.1016/j.ajhg.2015.09.007.
31. Ikeda Y, et al. Spectrin mutations cause spinocerebellar ataxia type 5. Nat Genet. 2006;38:184–190. https://doi.org/10.1038/ng1728.
32. Lise S, et al. Recessive mutations in SPTBN2 implicate β-III spectrin in both cognitive and motor development. PLoS Genet. 2012;8:e1003074. https://doi.org/10.1371/journal.pgen.1003074.
33. Lieto M, et al. The complex phenotype of spinocerebellar ataxia type 48 in eight unrelated Italian families. Eur J Neurol. 2020;27:498–505. https://doi.org/10.1111/ene.14094.
34. Depondt C, et al. Autosomal recessive cerebellar ataxia of adult onset due to STUB1 mutations. Neurology. 2014;82:1749–1750. https://doi.org/10.1212/WNL.0000000000000416.
35. Synofzik M, et al. Phenotype and frequency of STUB1 mutations: next-generation screenings in Caucasian ataxia and spastic paraplegia cohorts. Orphanet J Rare Dis. 2014;9:1–8. https://doi.org/10.1186/1750-1172-9-57.
36. Minnerop M et al. Hypomorphic mutations in POLR3A are a frequent cause of sporadic and recessive spastic ataxia. Brain. 2017;140:1561–1578. https://doi.org/10.1093/brain/awx095.
37. Paolacci S et al. Specific combinations of biallelic POLR3A variants cause Wiedemann–Rautenstrauch syndrome. J Med Genet. 2018;55:1–10. https://doi.org/10.1136/jmedgenet-2018-105528.
38. Coppieters F, Lefever S, Leroy BP, De Baere E. CEP290, a gene with many faces: mutation overview and presentation of CEP290base. Hum Mutat. 2010;31:1097–1108. https://doi.org/10.1002/humu.21337.
39. Frank V, et al. Mutations of the CEP290 gene encoding a centrosomal protein cause Meckel-Gruber syndrome. Hum Mutat. 2008;29:45–52. https://doi.org/10.1002/humu.20614.
40. Régal L, et al. Mutations in PEX10 are a cause of autosomal recessive ataxia. Ann Neurol. 2010;68:259–263. https://doi.org/10.1002/ana.22035.
41. Yamashita T, et al. Ataxic form of autosomal recessive PEX10-related peroxisome biogenesis disorders with a novel compound heterozygous gene mutation and characteristic clinical phenotype. J Neurol Sci. 2017;375:424–429. https://doi.org/10.1016/j.jns.2017.02.058.
42. Yoo DH, et al. Identification of FASTKD2 compound heterozygous mutations as the underlying cause of autosomal recessive MELAS-like syndrome. Mitochondrion. 2017;35:54–58. https://doi.org/10.1016/j.mito.2017.05.005.
43. Ghezzi D, et al. FASTKD2 nonsense mutation in an infantile mitochondrial encephalomyopathy associated with cytochrome C oxidase deficiency. Am J Hum Genet. 2008;83:415–423. https://doi.org/10.1016/j.ajhg.2008.08.009.
44. Wei X, et al. Mutations in FASTKD2 are associated with mitochondrial disease with multi-OXPHOS deficiency. Hum Mutat. 2020;41:961–972. https://doi.org/10.1002/humu.23985.

45. Popow J, Alleaume AM, Curk T, Schwarzl T, Sauer S, Hentze MW. FASTKD2 is an RNA-binding protein required for mitochondrial RNA processing and translation. RNA. 2015;21:1873–1884. https://doi.org/10.1261/rna.052365.115.

ACKNOWLEDGEMENTS

This work was in part supported by the patients' association "Connaître les Syndromes Cérébelleux" (CSC).

AUTHOR CONTRIBUTIONS

Conceptualization: M.B., M.K. Data curation: M.B., M.K., C. Guissart. Formal analysis: M.B., M.K., C. Guissart. Y.H., L. Larrieu. M.P., C.L.H. Funding acquisition: M.K., C. Guissart. Investigation: M.B., C.M., A. Roubertie. E.O., A. Choumert. F.F., F.O.M., M.R., I.B., O.P., J.M.R., D.C.S., C.S., X.A., A. Rolland. R.M., B.L., C.T. E. Bernard. M.M., C.C.D., C.T., P.M., L.D., L.P., C.A., A. Chaussenot. B.I., K.N., W.C., A.E., N.C., A. Riquet. E.T., V.G., E.C., S.A., S.O., A. Castrioto. C.E., P.C., L.K., S.S., N.B.B., E.K., A.D., B.D., S.J., G.R., V.F., L.A.H., L. Lazzaro. V.L., F.V., C. Charlin. S.F., M.C.M., T.W., C.F., U.W.L., M.F., B.C., J.F., E. Bieth. G.C., S.V., I.M., A.V., E.B.B., C. Coubes. D.G., N.L., J.P.A., M.A., C. Goizet. F.R., P.L., P.C. Methodology: M.B., M.K. Project administration: M.K. Resources: M.K. Software: D.B. Supervision: M.K. Validation: M.K., C. Guissart. M.B. Visualization: M.B., M.K., C.M. Writing—original draft: M.B., M.K. Writing—review & editing: M.B., M.K.

ETHICS DECLARATION

This study was approved by the "Comité de Protection des Personnes (CPP) Est IV–Strasbourg" ethic committee (number 02/115, study promotor HUS number 2863). Study authorization number DGS2003/0016. All patients signed a written consent before genetic analysis.

COMPETING INTERESTS

The authors declare no competing interests.

Correspondence and requests for materials should be addressed to M.K.